PREDICTED FUEL-SAVINGS FOR A FLETTNER ROTOR ASSISTED TANKER USING COMPUTATIONAL FLUID DYNAMICS

L Jones and M Prince, Wolfson Unit M.T.I.A., UK D Hudson, University of Southampton, UK J Cocks, Shell Shipping and Maritime, UK

SUMMARY

This paper presents a case study of the effectiveness of Flettner rotors as a wind-assist system for tanker hull forms with particular focus on the aerodynamic modelling of the devices. It summarises a series of computation fluid dynamics simulations carried out to evaluate the impact of parametric changes in Flettner rotor design, including the impact of multiple rotors operating in combination, and the influence of the ship induced flow field. The results of these simulations have been applied within a velocity performance prediction approach to estimate reductions in thrust required from the propeller, and hence changes in engine power and fuel consumption in realistic operations. The analysis highlights Flettner rotors as a means of providing significant levels of power assistance dependent upon true wind speed, heading and ship speed.

NOMENCLATURE

-	
	end-plate and the diameter of the main
	rotor body
C_D	Drag coefficient
C_L	Lift coefficient
C_M	Moment or torque coefficient
D	Rotor diameter (m)
E	Rotor efficiency
L	Rotor lift (N)
P_r	Power required to rotate a rotor (W)
P_t	Thrust power produced by a rotor (W)
U	Free-stream velocity (m/s)
VPP	Velocity Prediction Program
VR	Velocity Ratio: Circumference
	velocity/wind speed (-)

Ratio between the diameter of the rotor

1. INTRODUCTION

The recent increase in the use of Flettner rotors on commercial vessels has been supported by an increase in the activity of researchers in aerodynamic numerical and experimental modelling, eg. [1] and [2].

The objective of this research was to extend numerical modelling and assessment tools to aid performance predictions in terms of wind assisted powering of ships with Flettner rotors, with some approaches being transferrable to the assessment of other shipborne wind assistance systems. To this end, the performance of full scale Flettner rotors has been investigated using computational fluid dynamics (CFD) for a variety of wind conditions, geometries and placement scenarios, with the intention of demonstrating factors that may affect rotor performance in real-world installations. Results from the CFD analysis were then incorporated into a performance prediction model to assess potential power savings, taking into account factors such as the aero/hydrodynamic resistance of the vessel and expected wind conditions.

2. COMPUTATIONAL FLUID DYNAMICS METHODOLOGY

CFD simulations were conducted on the IRIDIS 5 supercomputer at the University of Southampton using the OpenFOAM toolbox, with details as follows:

- Simulations were conducted using an unsteady Reynolds averaged Navier-Stokes (URANS) based transient solver.
- The rotor was modelled as rotating by specifying a moving-wall boundary condition.
- Simulations were conducted at 1:1 scale, hence at full-scale Reynolds numbers (up to 5x10⁶).
- Simulations were conducted with a minimum domain size of 80 rotor diameters wide by 100 rotor diameters long by 24 rotor diameters high.
- The air was assumed to be 15 degrees Celsius.
- Turbulence effects were accounted for using a kappaomega SST turbulence model, with the viscous sublayer modelled using wall functions.

The simulations are comparatively expensive in computational terms due to the nature of the problem. The flow around the rotor is an unsteady bluff body flow, and hence the required temporal integration for the simulations scales with the number of flows past the cylinder (i.e. D/U). Conversely, because the surface velocity of the cylinder is typically multiples of the freestream velocity, the mesh resolution near the wall must be fine and the time step small relative to the temporal integration length. Ultimately, these conflicting requirements mean that the simulations require considerably more computational expense than flow past, for example, a static cylinder, wing or conventional sailing yacht rig. Therefore, whilst a case could be made for using large or direct eddy simulation (LES or DES) due to the bluff-body flow physics present, this is precluded for reasons of pragmatism, since these methods would be prohibitively computationally expensive for the parametric analysis conducted here.

Each simulation was run for at least 24 hours using 32 processors, and a total of 104 simulations have been conducted, resulting in 80,000 processor hours in total. Simulations typically used nominally 20 million cells per rotor.

3. ANALYSIS OF BASELINE ROTOR GEOMETRY

A 'baseline' rotor geometry is defined as possessing diameter 5m and height 30m, with a rotating end-cap (or so-called 'Thom disk') possessing twice the rotor diameter (i.e. C=2). This rotor geometry is intended to represent the scale appropriate to large vessels, e.g. of the order of 200m LWL. Unless otherwise specified, for example when investigating the effect of geometry changes, all simulations use the baseline rotor geometry. The effect of wind speed and rotation rate is investigated by simulating the baseline Flettner rotor geometry at a range of realistic wind speeds and rotation rates. The rotation rate was varied between a minimum of 50RPM and a maximum of 236RPM, however all results are presented in terms of the velocity ratio, VR, defined as the tangential velocity at the rotor surface divided by the free-stream velocity. The inflow condition was specified as a uniform velocity distribution, and a visual example is provided in Figure 1. Plotting the results in dimensional form (Figure 2), illustrates that as the wind speed increases the forces acting upon the rotor, as well as the torque required to drive the rotor, increase significantly. Plotting these results in coefficient form collapses them to nominally a single curve each (Figure 3 & 4), broadly independent of wind speed and dimensional rotation rate. This means that results can be scaled to predict rotor performance at other wind speed and velocity ratios, for example when conducting route analysis.

The L/D ratio of the rotor reaches a maximum at a low velocity ratio in the range, 1 < VR < 2, and then decreases with increasing velocity ratio, however L/D is not an especially illuminating quantity in terms of quantifying rotor performance for ship propulsion. In this context, the rotor efficiency, defined as the thrust power produced by the rotor divided by the rotational power required to drive it, is perhaps the most important metric. Under normal operating conditions a Flettner rotor will produce more power than required to drive it, hence this parameter may also be thought of as a power multiplication factor, and the terms are used interchangeably here. When referring to rotor efficiency, it should be noted that thrust power is a function of apparent wind speed and direction, and hence can only be determined in the context of a rotor on a vessel travelling at a known speed, with known wind conditions. For the purposes of assessing rotor performance in isolation, a pseudo power multiplication factor can be defined as $E=LU/P_r$, with L the rotor lift and U the freestream velocity. This quantity is a maximum at the smallest velocity ratio tested, and then decreases with increasing velocity ratio (figure 5). For the baseline rotor configuration, E=1 occurs at a velocity ratio of 10. This means that below a velocity ratio of 10, the rotor will always provide more thrust energy than it consumes in order to rotate it. However, when considering this result it should be borne in mind that the flow conditions investigated via CFD are similar to a rotor in optimum conditions – e.g. a beam reach, whereas in practice a proportion of the lift will be delivered as sideforce instead of thrust. The precise amount will vary depending upon wind angle, however the effect will be to reduce the cutoff point (in terms of velocity ratio) at which the rotor becomes uneconomical.

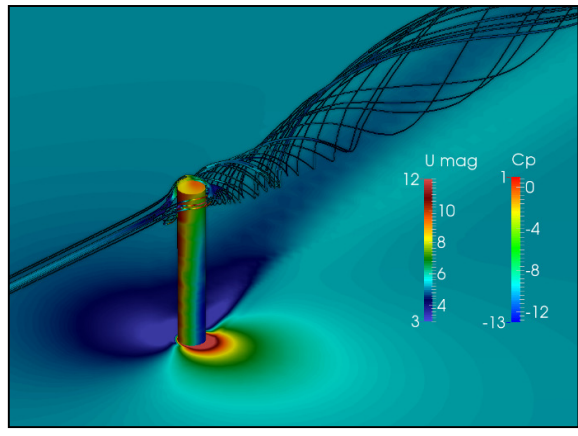


Figure 1: Illustration of a Flettner rotor with no end-cap in a uniform flow. The rotor is coloured by pressure coefficient, the near-wall plane is coloured by velocity magnitude, and streamlines are shown illustrating the vortex originating at the rotor tip

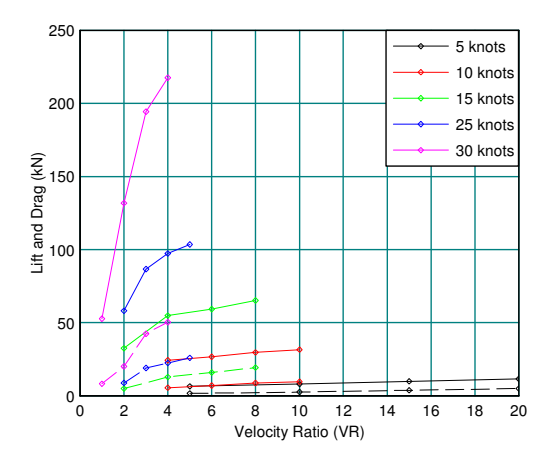


Figure 2: Variation of lift (solid) and drag (dashed) with velocity ratio for the baseline rotor

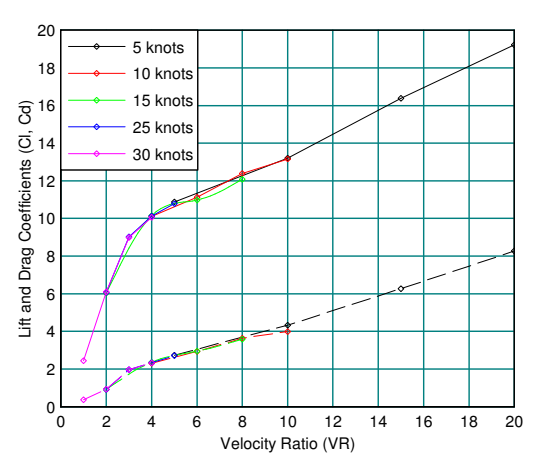


Figure 3: Variation of lift coefficient (solid) and drag coefficient (dashed) with velocity ratio for the baseline rotor

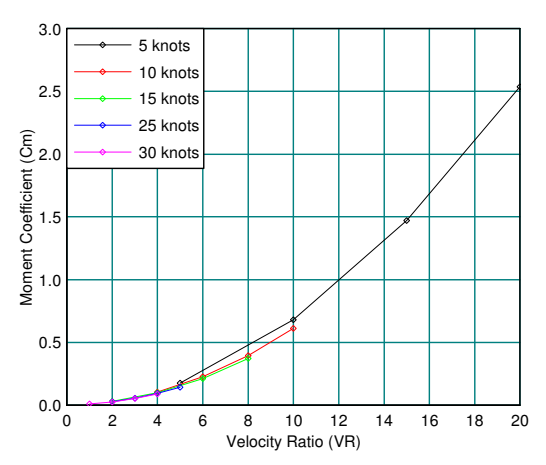


Figure 4: Variation of moment coefficient with velocity ratio for the baseline rotor

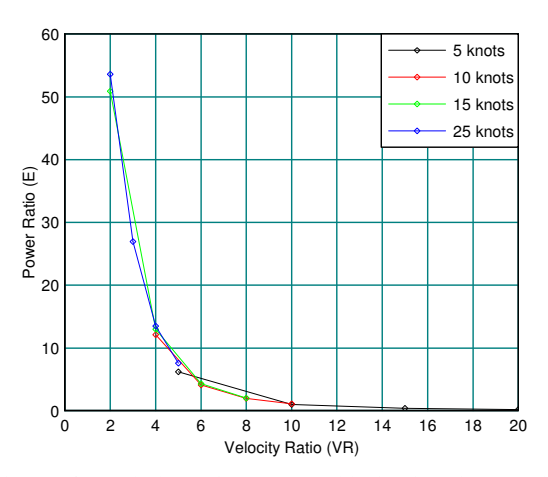


Figure 5: Variation of power multiplication factor with velocity ratio for the baseline rotor

4. INFLUENCE OF ASPECT RATIO

The influence of aspect ratio upon rotor performance is investigated by simulating a series of Flettner rotors possessing different heights and diameters, all subject to a uniform 15 knot wind profile at velocity ratios of 2, 4, 6 and 8, and possessing an end-cap diameter ratio of 2.

The effect of increasing rotor aspect ratio is to decrease the drag coefficient significantly, increase the lift coefficient slightly (Figure 6), and to decrease the torque coefficient (Figure 7). The net effect is that the power multiplication factor increases with increasing aspect ratio (Figure 8) meaning that, ignoring all other factors and constraints, the ideal shape for a Flettner rotor is as large an aspect ratio (i.e. as tall and slender) as possible. It should be noted however that the benefit of increasing aspect ratio decreases as the aspect ratio increases – the rotor performance asymptotes to the 'ideal' situation of an infinite aspect ratio.

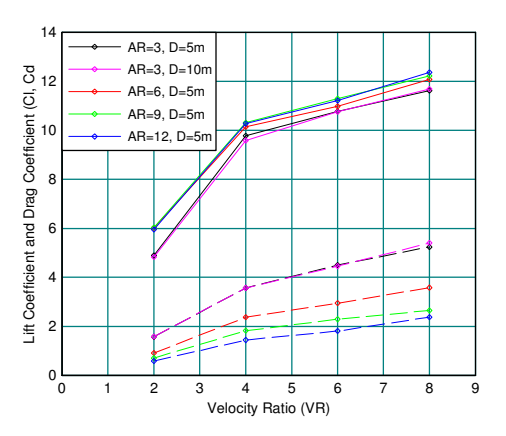


Figure 6: Variation of lift (solid) and drag (dashed) coefficients with velocity ratio for rotors posessing differing dimensions

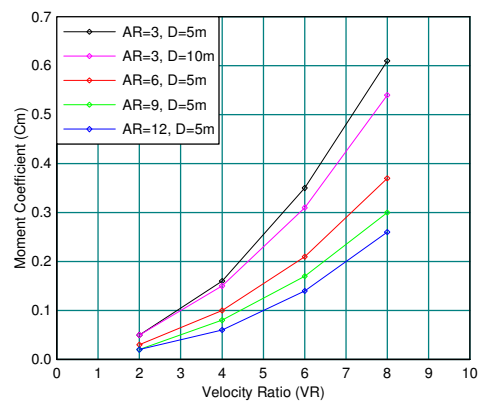


Figure 7: Variation of moment coefficient with velocity ratio for rotors posessing differing dimensions

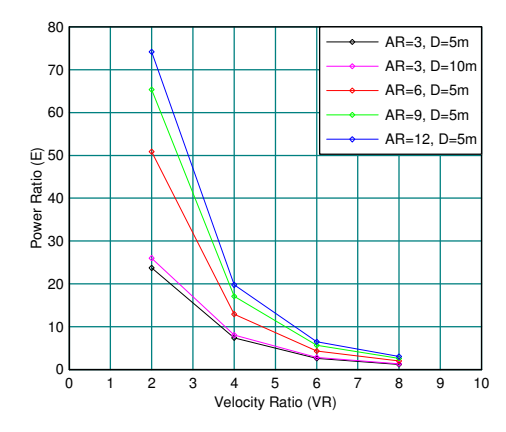


Figure 8: Variation of power multiplication factor with velocity ratio for rotors posessing differing dimensions

5. INFLUENCE OF ROTOR END PLATE

Earlier studies on Flettner rotors report that the addition of an end plate (or 'Thom disk') to the end of a rotor can decrease the rotor drag and will increase the rotor lift [3]. This effect is investigated for a full scale rotor by varying the relative size of the end-plate whilst keeping the thickness constant. The end plate diameter ratio is increased from C=1 (i.e. no end-plate) to C=4, for which simulations were conducted at a single windspeed of 15 knots and velocity ratio of 6. It can be seen in Figure 9 that as the end-plate diameter increases from C=1 to C=2 the drag coefficient increases to a maximum before dropping with further increases in plate diameter, whereas the lift coefficient exhibits a step-change increase between C=1.5 and C=1.75, and then a more gradual increase with further increases in end plate diameter. Perhaps most importantly, the moment coefficient increases significantly with increasing end plate diameter, and so the power multiplication factor decreases monotonically (Figure 10). These results imply that, whilst increasing the end-plate diameter increases lift significantly, particularly when moving to C=1.75-2, it also reduces the rotor efficiency, even for the smallest disc tested (C=1.25). This is because as the disc diameter increases, not only does the surface area of the disc increase proportional to the diameter squared, but the edge velocity of the disc increases proportional to the disc diameter, resulting in a compound increase in skin friction and hence torque required to drive the rotor. These results appear to suggest that a rotor with no end-plate is the most efficient, although not the most powerful, design. The question therefore arises as to whether holding the end-plate stationary (i.e. nonrotating), whilst operating the rotor will lead to an increase in rotor efficiency. In order to investigate this, simulations of the baseline rotor geometry were conducted with a static end-plate (C=2), and are plotted in Figure 10.

The effect of holding the end-plate stationary is to reduce the lift and drag coefficients slightly, but to significantly reduce the moment coefficient. The net effect is a large increase in the power multiplication factor, nominally by a factor of two at C=2, as noted by [4]. In fact, the effect of holding the end-plate stationary is to increase the power ratio over and above that observed for the rotor with no end-plate (E=9.1 as compared to E=8.1 at VR=6). These results represent the highest power multiplication factors observed for all end-plate geometries tested. The CFD analysis therefore predicts a clear performance benefit of holding the end-plate stationary, however the drawback to this approach would be the increased system complexity required to hold the end-plate static.

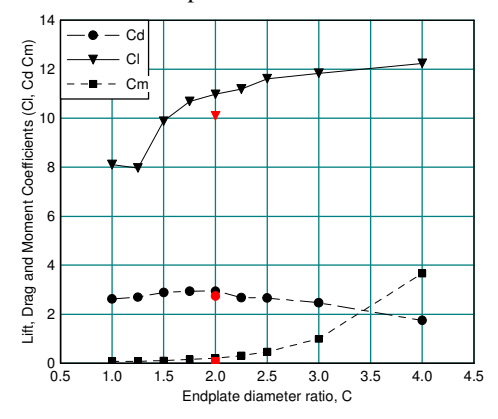


Figure 9: Variation of lift, drag and moment coefficients with endplate diameter ratio for rotating (black) and static (red) end plates

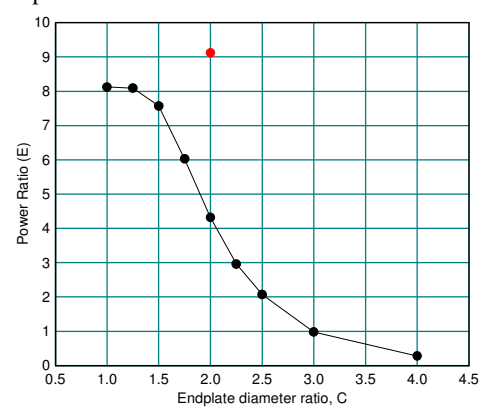


Figure 10: Variation of power ratio with endplate diameter ratio for rotating (black) and static (red) end plates

6. INTERFERENCE EFFECTS OF MULTIPLE ROTORS

The influence of rotor separation is investigated by conducting simulations of a pair of Flettner rotors and varying the separation distance and separation vector. Simulations have been conducted translating the rotors both in the streamwise (*x*) and lateral (*y*) directions, with the rotor axes separated by 2.5, 3, 4 and 6 rotor diameters (i.e. 12.5, 15, 20 and 30m). All simulations were conducted with a free-stream velocity of 15 knots and nominal velocity ratio of 6.

Figures 11 and 12 show that for all cases the mean drag coefficient is higher than that of a single rotor and the mean lift coefficient is lower than for a single rotor.. Accordingly, the mean power multiplication factor is also lower than for a single rotor (Figure 13). This means that

the net effect of rotor interference is to reduce system performance. The behaviour of the rotors differs depending on whether the rotor separation is in the streamwise or lateral directions, however.

When the rotor separation is in the streamwise direction (Figure 15), the drag acting on the rotors is the most significantly affected quantity, with the downstream rotor exhibiting significantly increased drag, and the upstream rotor significantly decreased drag. Inspecting contours of pressure at the midplane suggests that this is because the location of minimum pressure (i.e. suction) moves slightly toward the downstream side of the downstream rotor, and to the upstream side of the upstream rotor, as compared to the case of a rotor in isolation. Lift is also affected (reduced), but less significantly. The overall system performance appears to be particularly sensitive to streamwise separation, because even at the largest separation tested (30m centre-to-centre) the mean power multiplication ratio had not recovered to that of a single rotor, being 10% lower, and the mean drag was still 50% higher than for a single rotor.

When the rotor separation is in the lateral direction (Figure 16) it is the lift produced by the rotors that is affected most significantly, with the rotor on the high speed/suction side exhibiting dramatically increased lift, but the rotor on the low speed/pressure side exhibiting dramatically decreased lift. This appears to be because the superposition of rotor flows increases the maximum velocity in the vicinity of the rotor on the high speed side, but decreases it on the low speed side (compare Figures 14 to 16). The mean lift, however, is close to that of a single rotor. The performance of laterally spaced rotors appears less sensitive than for streamwise spacing, because by 30m spacing the mean power multiplication factor had returned to that of a single rotor, although the mean drag coefficient was still 30% higher. This is in keeping with [2] identifying that drag coefficient is sensitive to changes in pressure distribution. These results show that rotor performance can be strongly affected by interference effects, particularly for rotors aligned in the streamwise direction. It is clear that rotors should ideally be placed as far away from one another as possible, and it is conceivable that there may be merit in considering locating rotors in, for example, a staggered pattern.

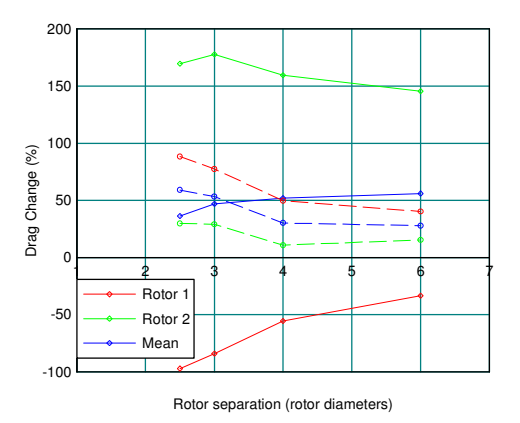
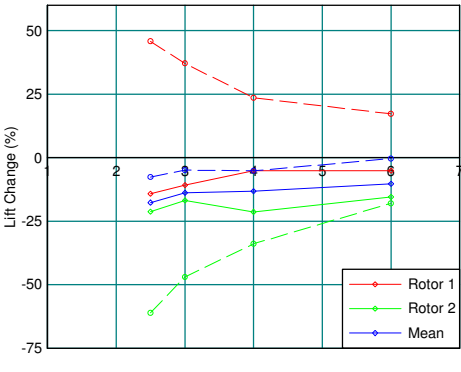


Figure 11: Drag change as a function of longitudinal (solid) and lateral (dashed) rotor separation, relative to a rotor in isolation



Rotor separation (rotor diameters)

Figure 12: Lift change as a function of longitudinal (solid) and lateral (dashed) rotor separation, relative to a rotor in isolation

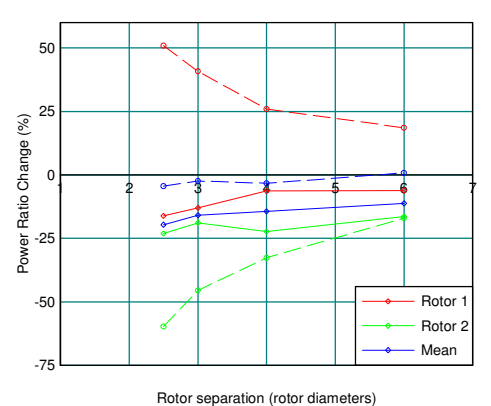


Figure 13: Power ratio change as a function of longitudinal (solid) and lateral (dashed) rotor separation, relative to a rotor in isolation

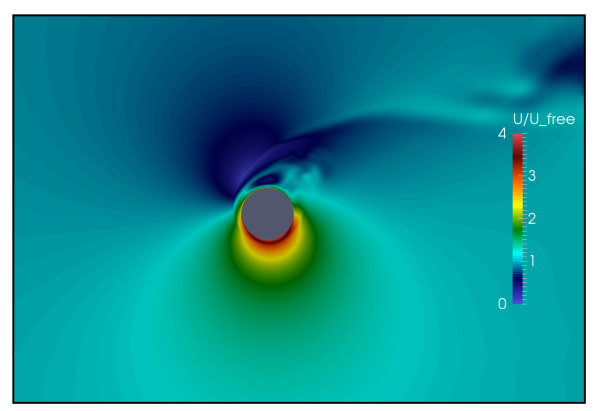


Figure 14: Velocity ratio plotted at the mid-height for a single rotor at U=15 knots and VR=6

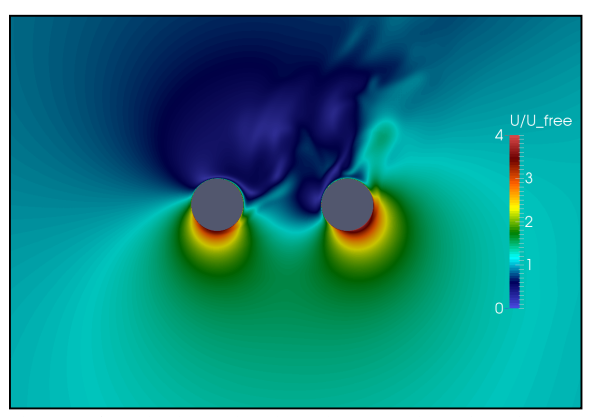


Figure 15: Velocity ratio plotted at the mid-height for two rotors with a streamwise separation of 7.5m, at U=15 knots and VR=6

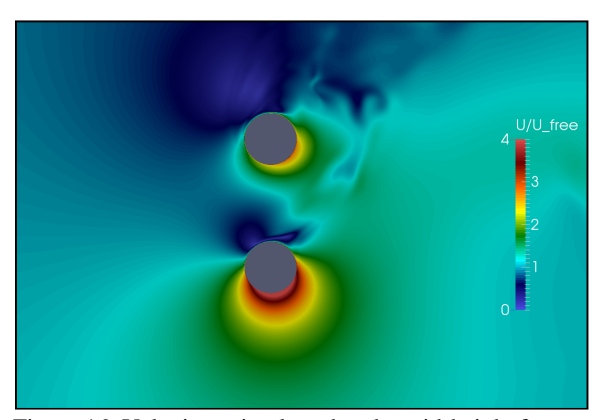


Figure 16: Velocity ratio plotted at the mid-height for two rotors with a lateral separation of 7.5m, at U=15 knots and VR=6

7. INFLUENCE OF SUPERSTRUCTURE PROXIMITY

The influence of nearby superstructure is investigated by conducting simulations of a rotor in proximity to a cuboid obstacle, i.e. a box, representing a generic superstructure element causing a flow blockage. The box possesses width 30m, depth 10m and height 10m, and is placed with the long side facing the rotor. A three dimensional view of the configuration is provided in Figure 17. The rotor and box were simulated for a range of separation distances and blockage angles around the rotor. The angles are defined such that 0 degrees is immediately upstream of the rotor, 90 degrees is beside the rotor, on the high speed/suction side, and 270 degrees is beside the rotor on the low speed/pressure side. All simulations were conducted with a free-stream velocity of 15 knots and velocity ratio of 6. When the separation gap is small, i.e. one rotor diameter (or 5m), the rotor lift does not ever exceed that of a rotor in isolation irrespective of obstacle orientation relative to the rotor. Therefore the presence of a nearby obstacle acts only to degrade rotor performance (Figure 18). The rotor efficiency performance is most severely degraded when the obstacle is directly upstream of the rotor (0 deg.), and at +/-45 deg. upstream either side of the rotor centreline. The performance is also degraded significantly, but to a lesser extent, when the obstacle lies downstream of the rotor. These results suggest that, if it is desired to optimise the performance of a vessel for reaching conditions, it is preferable for superstructure to be located fore or aft of a Flettner rotor as opposed to on the port or starboard side. The effect of varying the distance of the box from the rotor was investigated for lateral placements only (i.e. +/- 90 degrees). The results (Figure 19) suggest that placing an obstacle on the pressure side of the rotor at close proximity is more harmful than placing an obstacle on the suction side of a rotor. However, the performance detriment decreases rapidly as the box is moved further away, and in fact an efficiency increase of nominally 5% is reported at a separation gap of three rotor diameters (15m).

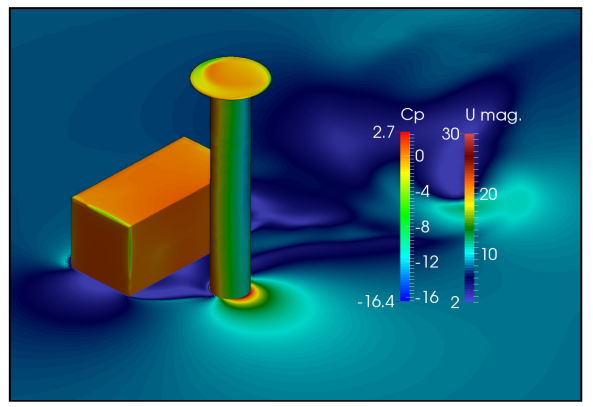


Figure 17: Image of a Flettner rotor with box located on the pressure/low velocity side. The rotor is coloured by the pressure coefficient, whilst the near-wall plane shows the velocity magnitude. The air is flowing from the bottom-left to the top-right of the image.

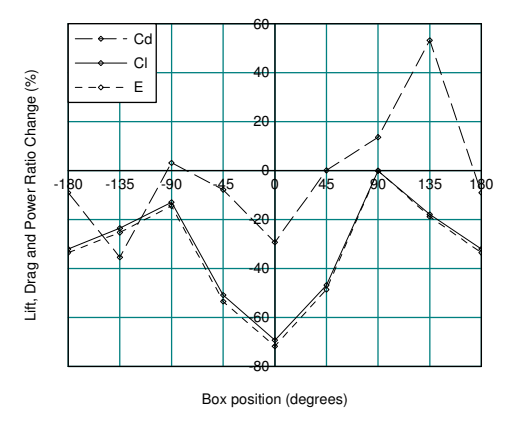


Figure 18: Drag, lift and efficiency change as a function of box orientation, for a separation gap of one rotor diameters, relative to a rotor in isolation

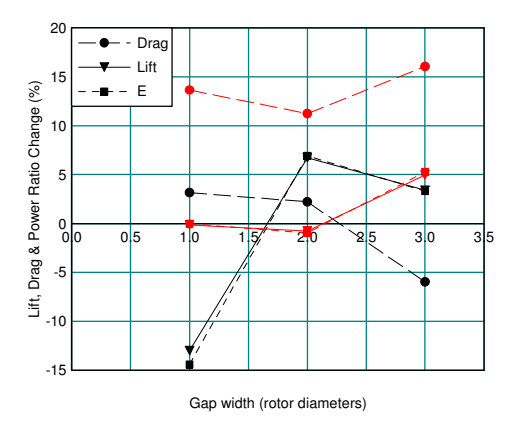


Figure 19: Drag, lift and efficiency change as a function of a separation gap width for a box on the pressure side of the rotor (black) and on the suction side of the rotor (red), relative to a rotor in isolation

8. INFLUENCE OF SITING UPON A SHIP HULL

The influence of locating a Flettner rotor on a ship form, as opposed to on a flat surface, is investigated by simulating a single rotor on a simple ship geometry, without superstructure, at a variety of wind angles, at a wind speed of 15 knots and velocity ratio of 6. The detail of the ship form is not critical, it is rather the blockage effect of the vessel on the wind flow that is important. To this end, a generic hullform was created, possessing 200m LOA, 40m beam and 10m freeboard. The rotor was located nominally 45m from the bow and 15m from the centreline of the vessel, and the complete configuration is illustrated in Figure 20. The wind angles are defined such that 0 degrees corresponds to flow from bow to stern, and 90 degrees corresponds to flow from port to starboard.

The effect of including the ship structure is to introduce a secondary flow pattern which interacts with the flow around the Flettner rotor. Effectively the ship creates a blockage (modified flow field) which, particularly for wind angles of +/-90 degrees, creates a large region of flow separation, comprising a slower moving region of air over the deck and downstream of the vessel (Figure 21) and encompassing the Flettner rotor. Where the wind angle is 0 or 180 degrees the ship imparts a significantly smaller blockage to the flow, and the Flettner rotor does not sit within a low speed/separated region of flow (Figure 22).

The net effect of the ship presence is to reduce the rotor efficiency at all points of sail, as seen from Figure 23. The rotor efficiency is lowest at +/-90 degrees, and -135 degrees, which are angles at which the ship presents a large frontal area to the flow, and creates the largest wake over the deck. At these angles since the rotor lies in a region of decelerated flow, the effective velocity ratio of the rotor increases, causing the efficiency of the rotor to decrease in line with the trends identified in section 2. When the ship is orientated at 0 or 180 degrees the rotor does not lie in a large separated region and the rotor efficiency is correspondingly higher, however since the

Magnus effect produces thrust perpendicular to the wind direction, the Flettner rotor would not produce useable thrust under these conditions. These results indicate that in practice the flow around a rotor installed on a ship may differ significantly from simple uniform or power law boundary layers. In particular, reaching (true wind angles of the order of 90°) conditions may lead to the flow over the rotor being decelerated, which may potentially require the use of a lower rotation rate in order to maintain a velocity ratio corresponding to efficient rotor operation.

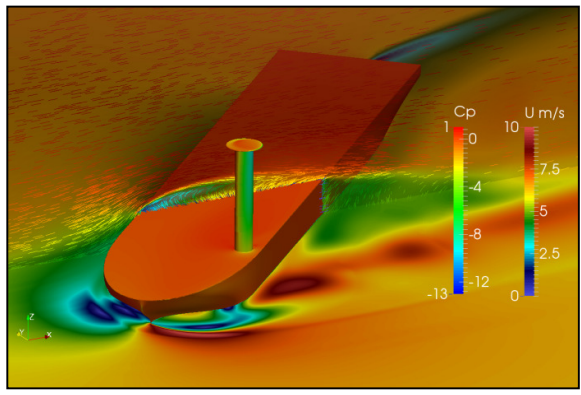


Figure 20: View of a simple ship hull with Flettner rotor, with wind angle of -45 degrees. The rotor and ship hull are coloured by pressure coefficient, whilst the near-wall plane is coloured by velocity magnitude.

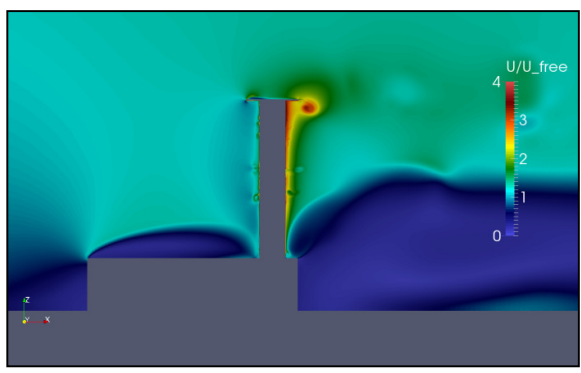


Figure 21: Non-dimensional velocity plotted on a plane through the centre of a rotor located on a simple ship, for a flow angle of 90 degrees at U=15knots and VR=6. The air is flowing from left to right.

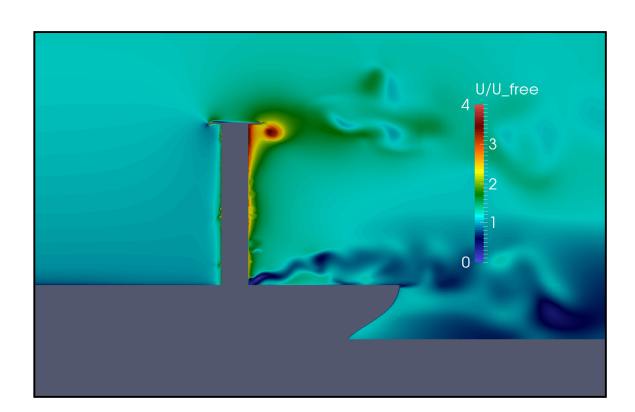


Figure 22: Non-dimensional velocity plotted on a plane through the centre of a rotor located on a simple ship, for a flow angle of 180 degrees at U=15knots and VR=6. The air is flowing from left to right.

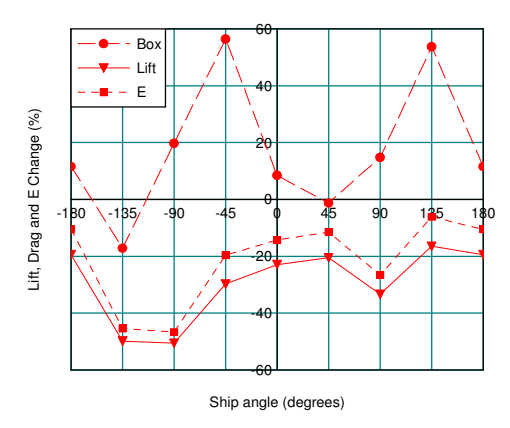


Figure 23: Drag, lift and efficiency change as a function of wind direction for a rotor mounted on a generic ship hullform, relative to a rotor in isolation.

9. COMMENTS ON OPTIMAL ROTOR SPECIFICATIONS

When considering a Flettner rotor installation on a vessel one of the most critical questions regards what height and diameter should the rotors should be. It has been demonstrated that rotors with high aspect ratios are more efficient, however in practice the maximum height of a rotor installation is likely to be limited by the requirement to navigate underneath bridges. Assuming that the rotor height is fixed by operational or structural considerations, the next dimension to specify is the rotor diameter. Increasing the rotor diameter for a fixed rotor height has a number of effects. For example, as diameter is increased the efficiency of the rotor decreases but the absolute lift produced by the rotor increases. Clearly a very efficient rotor is not practical if it cannot produce a meaningful amount of lift, and likewise a powerful rotor is not practical if it is inefficient, but between these extremes there is a viable range of rotor diameter. Furthermore, as the rotor diameter increases the drag of the rotor also increases, meaning that during time periods when wind conditions are not favourable the rotor will represent a bigger detriment to vessel efficiency. Therefore, it is likely that the greater percentage of time a vessel is expected to experience favourable wind conditions, the larger the optimum rotor diameter may be. It is clear then, that the optimum rotor dimensions and placement are likely to depend upon the size and speed of the vessel, as well as the particular route(s) navigated, and hence wind conditions experienced, by the vessel. So in practice, whilst the analysis of Flettner rotors in isolation can illustrate behavioural trends, any optimisation of parameters such as rotor diameter or spatial placement cannot be achieved by considering the performance of rotors in isolation. In order to optimise the various aspects of a rotor installation a system-wide approach must be

undertaken, considering both the hydrodynamic and aerodynamic performance of both the vessel and rotor installation, as well as the drivetrain performance and, critically, the route and expected wind conditions experienced by the vessel.

10. CASE STUDY

In order to assess the impact of differences in rotor performance, two types of generic ship form are evaluated; a LNG carrier and a LR2 tanker. Principal dimensions of these vessels are provided in Table 1.

A number of configurations were taken from the CFD analysis described previously and a selection of them are detailed in Table 2.

		LNG	LR2
LOA	m	276	245
Bmax	m	46	42
Т	m	11.4	15.475
Displacement	tonnes	105000	125000
Freeboard	m	14.5	14

Table 1: Principal vessel parameters

Configuration	Units	Α	В	С	D	Е	F
Ship Type		LNG	LNG	LNG	LNG	LR2	LR2
Aspect Ratio		6	9	4.17	6	6	6
No. of rotors		4	4	4	4	4	2
Rotor Height	m	30	36.67	25	25	30	30
Rotor Diameter	m	5	4.08	6	4.17	5	5
Rotor Limit	rpm	180	221	150	216	180	180
Single Ref. Area	m^2	150	150	150	104.2	150	150
Total Ref. Area	m^2	600	600	600	416.7	600	300

Table 2: Modelled rotor configuration details

11. PERFORMANCE PREDICTION

In order to assess the aerodynamic performance impact resulting from CFD generated data a velocity performance prediction (VPP) approach was used. A simplified assessment approach was selected yielding results in terms of power saving, i.e. % reduction in delivered engine power. It is noted that other authors have tackled some of these aspects in more detail, as can be seen in ref [1].

An existing sailing yacht based VPP, Wolfson Unit 'WinDesign' was modified and used for this case study. This amalgamates force and moment contributions from the hydrodynamic and aerodynamic components and solves for the ship speed and associated stability for a range of true wind speeds, headings, engine and rotor contributions. The basic sailing aspects of this are in keeping with [5].

11.1 HYDRODYNAMIC FORCE MODELLING

The hydrodynamic force model main components were as follows:

$$R_T = R_U + R_H + R_I - T_P$$

- R_T: total hydrodynamic resistance
- R_U: upright resistance; based on the power prediction for single screw merchant ships from the Wolfson Unit Powering Program (calm water predictions).
- R_{H:} resistance due to heel based on a regression of in-house model tank data of ship forms in a 'sailing' condition.

- R_E induced drag based on a regression of inhouse model tank data of ship forms in a 'sailing' condition.
- Tp: Thrust from drivetrain contribution

These were amalgamated into a hydrodynamic force model that was input into the VPP.

11.2 AERODYNAMIC FORCE MODELLING

The aerodynamic force model was created based on the previously presented CFD derived data. The majority of the simulations were carried out with a rotor in isolation and only a limited number with the rotor(s) located on the deck of the ship. The reductions in lift and increase in drag highlighted in sections 6 & 8 have been used to create factors to modify isolated rotor data to incorporate the ship induced and multiple rotor influences.

11.3 SOLUTION PHASE

This solution phase seeks the equilibrium between the aerodynamic and hydrodynamic longitudinal forces, transverse forces and roll moments at a range of true wind speeds and angles, engine thrust and rotor VR settings.

11.4 ASSUMPTIONS

In order to conduct this analysis a number of assumptions have been made, these include:

- A constant full load displacement condition was used for all simulations
- A rotational velocity limit of 180 rpm has been applied to 5m diameter rotors with proportional limits applied to other rotor diameters. All rotor data and limits are summarised in Table 2.
- Powering of the rotor(s) has been accounted for in the power saving calculations and efficiency factors have been applied in the conversion of effective to delivered power.
- Reduction of rotor performance due to siting on a ship geometry has been included, including the loss of lift and increase in drag highlighted in section 8.
- Performance coefficients used assume that the positioning of the rotor(s) will avoid significant adverse interactions.
- An aerodynamic windage model (including interactions with superstructure) of the rotors when not in use (i.e. when motoring upwind) has been included.
- Location of the rotor(s) and use of the vessel's hydrodynamic lift generating appendages to maintain a steady course has been ignored. It is acknowledged that it is vital to have yaw balance between the hydrodynamic and aerodynamic induced moments for the vessel to be able to sail.
- The impact of ship motions on the aerodynamic and hydrodynamic behaviour of the rotors have been ignored

11.5 RESULTS

The VPP analysis resulted in predictions of percentage power savings for specific constant ship speeds at a range of true wind speeds and angles. An example is presented in Table 4.

		True Wind Speed (knots)							
		5	10	15	20	25	30		
	0	-2.6	-5.0	-8.1	-11.3	-14.3	-16.9		
	10	-2.5	-4.9	-7.9	-11.1	-14.1	-16.7		
	20	-2.4	-4.7	-7.5	-10.5	-13.4	-16.0		
	30	-2.3	-4.3	-6.8	-9.6	-12.3	-14.8		
	40	-2.1	-3.8	-5.9	-8.3	-10.7	-13.1		
	50	-1.9	-3.2	-4.8	-6.7	-8.7	-10.8		
(gəp)	52	-1.8	-3.1	-4.6	-6.4	-8.3	-10.3		
e (c	60	-1.6	-2.6	-3.7	-5.0	-6.5	-8.1		
Angle	70	-1.4	-2.0	-2.6	-3.4	1.8	8.0		
ρι / pι	80	-1.2	-1.4	-1.4	9.0	26.8	31.4		
Wind	90	-1.0	-1.0	1.4	19.5	39.6	43.0		
True	100	-0.8	-0.6	4.9	27.9	47.6	65.4		
F	110	-0.6	-0.4	6.5	31.1	51.1	70.0		
	120	-0.5	-0.2	6.1	30.7	53.6	71.0		
	135	-0.3	-0.1	3.0	25.6	48.7	66.6		
	150	-0.3	0.0	0.2	15.5	39.3	59.4		
	160	-0.2	0.0	0.0	8.0	30.4	50.4		
	170	-0.2	0.0	0.0	1.5	20.2	39.5		

Table 3: Breakdown of percentage power savings for configuration A at constant 12 knots ship speed

11.6 ROUTE INFORMATION

Weather data used in this study is based on the summation of data recorded from a number of LNG carriers in operation over a 2 year period. This is representative of actual ship activities as it includes combinations of various routes, the true wind angle and speed distribution and is summarised in Table 4.

When combined with the VPP analysis it results in the power savings per configuration and steady ship speed ranges as presented in Table 5. These highlight the reduction in rotor propulsion assistance with increasing ship speed resulting from the decrease in apparent wind angle and associated reduction in thrust contribution, with no notable returns at 16 knots of ship speed or above.

The higher aspect ratio rotors, option B, provided a slight benefit (0.26%) in overall power reduction over the datum aspect ratio option (A).

There will be specific routes which would be more beneficial to the operation of rotors, those with predominantly strong winds (i.e. 20 knots and above) from 90° true wind or greater, reflected in the bottom right area of Table 3. This highlights the benefits of Flettner rotors as promising devices in practice for the immediate reduction in Greenhouse gas emissions from shipping.

		True wind speed (knots)						
		0-5	5-10	10-15	15-20	20-25	25-30	
(deg)	0-30	3.2	4.0	3.8	2.6	0.9	0.5	
	30-60	2.8	4.0	4.5	3.3	1.4	0.5	
Angle	60-90	1.3	3.6	5.3	4.2	2.7	1.0	
Wind,	90-120	1.1	2.7	4.7	3.8	2.3	1.2	
e W	120-150	1.6	3.0	3.6	4.2	2.3	1.4	
True	150-180	1.3	2.2	3.0	3.7	1.9	1.1	

		True wind speed (knots)						
		30-35	35-40	40-45	45-50	50-55	55-60	
(deg)	0-30	0.2	0.1	0.0	0.0	0.0	0.0	
р) ə	30-60	0.3	0.1	0.0	0.0	0.0	0.0	
Angl	60-90	0.4	0.1	0.1	0.0	0.0	0.0	
Wind Angle	90-120	0.4	0.2	0.1	0.0	0.0	0.0	
e ×	120-150	1.0	0.6	0.3	0.0	0.0	0.0	
True	150-180	0.6	0.4	0.2	0.1	0.0	0.0	

Table 4: Summary of applied route data

Ship Speed	Α	В	С	D	E	F
kts	LNG	LNG	LNG	LNG	LR2	LR2
8	-	-	-	-	12.60%	6.26%
10	8.34%	8.60%	7.89%	5.44%	8.29%	3.17%
12	4.68%	5.01%	4.42%	2.60%	4.48%	1.07%
14	2.03%	2.32%	1.94%	0.77%	1.81%	-0.09%
16	0.36%	0.52%	0.39%	-0.21%	0.21%	-0.57%
18	-0.67%	-0.62%	-0.51%	-0.65%	-0.68%	-0.66%
20	-1.03%	-1.08%	-0.86%	-0.71%	-0.96%	-0.57%

Table 5: Percentage power saving for a range of configurations

12. CONCLUSIONS

The behaviour of Flettner rotors has been investigated by conducting a series of CFD simulations.

It was determined that for a given wind speed, as the velocity ratio is increased the rotor lift, drag and torque all increase, however the rotor efficiency decreased. For the operating conditions simulated the results could be successfully collapsed to a single curve by plotting in non-dimensional coefficient form.

Rotor efficiency was found to increase with aspect ratio, however the optimum rotor dimensions for real-world installations must be determined by a holistic performance analysis, and are likely to be limited by operational constraints.

Adding a rotating end-plate to the rotor was found to increase the lift coefficient but decrease the rotor efficiency. Simulation results suggest that by holding the end-plate stationary, the efficiency can be improved above that of a rotor with no end-plate.

Where rotors are located in close proximity, the effect of the rotor interaction is to decrease the mean rotor performance. This effect is more pronounced where the rotors are orientated in the streamwise direction, where a power multiplication factor penalty of 10% was observed even at a separation of 6 rotor diameters.

Where a rotor lies in close proximity to a flow obstruction such as a box, the net effect is to decrease rotor performance. The performance penalty is largest where the obstacle is upstream of the rotor, and least when the obstacle lies either side of the rotor.

Where a rotor is located on a simple ship geometry, the flow experienced by the rotor can be significantly different to that of an ideal atmospheric boundary layer. In particular, where the free-stream flow lies at/close to 90 degrees the ship hull creates a large decelerated region of flow that may encompass the rotor. Decelerating the flow over the rotor increases the effective velocity ratio, and decreases the rotor efficiency.

The CFD results have been utilised within a VPP analysis process, resulting in predicted power savings of the order of 8% for a 4-rotor vessel at 10 knots based on actual averaged weather route information from vessel operations. The rotors are predicted to be ineffective as a propulsion assistance mechanism at 16 knots of ship speed or greater with these weather data applied.

13. ACKNOWLEDGEMENTS

The authors would like to thank Shell Shipping and Maritime for funding this project and giving permission for it to be published.

14. REFERENCES

- van der Kolk, N.J., Bordogna, G., Mason, J.C., Desprairies, P., Vrijdag, A. 'Case study: Windassisted ship propulsion performance prediction, routing, and economic modelling', RINA Conf. Power & Propulsion Alternatives for Ships, 2019.
- Bordogna, G., Muggiasca, S., Giappino, S., Belloli, M., Keuning, J.A., Huijmans, R.H.M., 'Experiments on a Flettner rotor at critical and supercritical Reynolds numbers', *Journal of Wind Engineering & Industrial Aerodynamics*, 2019.
- 3. Thom. A., 'On the effects of discs on the air forces on a rotating cylinder', *Reports and memoranda, Aeronautical Research Committee report 1623*, 1935.
- Badalamenti. C, 'On the application of rotating cylinders to micro air vehicles', *Doctoral Thesis* City University, 2010.
- 5. Oliver J.C., Claughton, A.R., 'Development of a multi-functional velocity prediction program (VPP) for sailing yachts', *RINA Intl Conf CADAP* '95, 1995.